Carbodithioate-Containing Oligo- and Polythiophenes for Nanocrystals' Surface Functionalization

Claudia Querner,*,† Alessandro Benedetto, Renaud Demadrille, Patrice Rannou, and Peter Reiss*

CEA Grenoble, Département de Recherche Fondamentale sur la Matière Condensée (DRFMC), SPrAM (UMR 5819-CEA/CNRS/UJF), Laboratoire d'Electronique Moléculaire, Organique et Hybride, 17 Rue des Martyrs, 38054 Grenoble Cedex 9, France

Received May 11, 2006. Revised Manuscript Received June 29, 2006

Organic ligands containing the chelating carbodithioate group are excellent candidates for the surface functionalization of various semiconductor and metal nanoparticles or flat substrates. We provide a simple synthetic scheme for the preparation of a series of regioregular oligo- and polythiophenes containing this functional group. In the first step, 3-[4-(bromomethyl)phenyl]-2,5-dibromothiophene is coupled either to 3-*n*-octylthiophene or to 3,3″-dioctyl-2,2′:5′,2″-terthiophene, leading to quasisymmetric thiophene trimers or heptamers, respectively. In the second step, these oligomers are submitted to oxidative polymerization, and finally the carbodithioic acid function is introduced. This procedure can be generalized for the preparation of a large number of functional oligo- and polythiophenes by simply varying the chemical structure of the thiophene precursors used. We illustrate the grafting of these compounds on the surface of CdSe nanocrystals with the example of 4-thiophen-3-yldithiobenzoic acid. Spectroscopic studies of the resulting thiophene-functionalized nanocrystals reveal photoinduced charge transfer at the organic/inorganic interface.

Introduction

Colloidal semiconductor nanocrystals have drawn a tremendous research interest, initiated by the possibility to prepare monodisperse size- and shape-controlled samples.[1] Basic and applied research in physics, chemistry, and materials science are devoted to these nano-objects, whose applications range from biological labeling[2] to photovoltaic devices and light-emitting diodes,[3] to name a few, using their size-tunable optical and electronic properties.[4]

A key step for most of these applications is the functionalization of the nanocrystals' surface with appropriate organic ligands, determining their dispersibility and enabling their binding to other molecules or substrates. Furthermore, the capping ligands can be of insulating, semiconducting, or conducting nature depending on their chemical structure and doping state. Therefore they play an important role in charge transfer processes between nanocrystals and their environment, which is of particular interest in optoelectronics and molecular electronics applications. From a chemical point of view, new ligands should have an anchor function with a high affinity for the nanocrystals' surface, allowing for the quasicomplete exchange with initial ligands under mild conditions. We have recently shown that the carbodithioate group is an interesting choice of an anchor function because it forms strong chelate-type bonds with "soft" metal atoms such as cadmium, lead, or gold.[5] By use of carbodithioate derivatives, electroactive aniline tetramer was grafted on CdSe nanoparticles, building a model system of a molecular hybrid between an organic and an inorganic semiconductor.

Here we present the synthesis and characterization of carbodithioate functionalized oligo- and polythiophenes, paving the way—after their grafting on the surface of semiconductor nanocrystals—for the fabrication of a new

* To whom correspondence should be addressed: e-mail peter.reiss@cea.fr (P.R.) or querner@sas.upenn.edu (C.Q.).

† Present address: David Rittenhouse Laboratory, Department of Physics and Astronomy, University of Pennsylvania, 209 S. 33rd St., Philadelphia, PA 19104.

(1) (a) Murray, C. B.; Norris, D. J.; Bawendi, M. G. *J. Am. Chem. Soc.* **1993**, *115* (19), 8706−8715. (b) Murray, C. B.; Kagan, C. R.; Bawendi, M. G. *Annu. Rev. Mater. Sci.* **2000**, *30*, 545−610. (c) Peng, X. G.; Manna, L.; Yang, W. D.; Wickham, J.; Scher, E.; Kadavanich, A.; Alivisatos, A. P. *Nature* **2000**, *404*, 59−61. (d) Manna, L.; Scher, E. C.; Alivisatos, A. P. *J. Am. Chem. Soc.* **2000**, *122* (51), 12700−12706. (e) Peng, Z. A.; Peng, X. G. *J. Am. Chem. Soc.* **2001**, *123* (7), 1389−1395. (f) Peng, Z. A.; Peng, X. G. *J. Am. Chem. Soc.* **2002**, *124* (13), 3343−3353. (g) Manna, L.; Milliron, D. J.; Meisel, A.; Scher, E. C.; Alivisatos, A. P. *Nat. Mater.* **2003**, *2* (6), 382−385.

(2) (a) Bruchez, M.; Moronne, M.; Gin, P.; Weiss, S.; Alivisatos, A. P. *Science* **1998**, *281*, 2013−2016. (b) Chan, W. C. W.; Nie, S. M. *Science* **1998**, *281*, 2016−2018. (c) Mattoussi, H.; Mauro, J. M.; Goldman, E. R.; Anderson, G. P.; Sundar, V. C.; Mikulec, F. V.; Bawendi, M. G. *J. Am. Chem. Soc.* **2000**, *122*, 12142−12150. (d) Michalet, X.; Pinaud, F. F.; Bentolila, L. A.; Tsay, J. M.; Doose, S.; Li, J. J.; Sundaresan, G.; Wu, A. M.; Gambhir, S. S.; Weiss, S. *Science* **2005**, *307*, 538−544.

(3) (a) Coe, S.; Woo, W.; Bawendi, M. G.; Bulovic, V. *Nature* **2002**, *420*, 800−803. (b) Lee, J.; Sundar, V. C.; Heine, J. R.; Bawendi, M. G.; Jensen, K. F. *Adv. Mater.* **2000**, *12* (15), 1102−1105. (c) Bakueva, L.; Musikhin, S.; Hines, M. A.; Chang, T. W. F.; Tzolov, M.; Scholes, G. D.; Sargent, E. H. *Appl. Phys. Lett.* **2003**, *82* (17), 2895−2897. (d) Konstantatos, G.; Huang, C.; Levina, L.; Lu, Z.; Sargent, E. H. *Adv. Funct. Mater.* **2005**, *15* (11), 1865−1869. (e) Huynh, W. U.; Dittmer, J. J.; Alivisatos, A. P. *Science* **2002**, *295*, 2425−2427. (f) Sun, B.; Snaith, H. J.; Dhoot, A. S.; Westenhoff, S.; Greenham, N. C. *J. Appl. Phys.* **2005**, *97* (1), 014914.

(4) (a) Weller, H. *Angew. Chem., Int. Ed. Engl.* **1993**, *32* (1), 41−53. (b) Woggon, U. *Optical Properties of Semiconductor Quantum Dots*; Springer: New York, 1997. (c) Gaponenko, S. V. *Optical Properties of Semiconductor Nanocrystals*; Cambridge University Press: Cambridge, U.K., 1998. (d) Bawendi, M. G.; Steigerwald, M. L.; Brus, L. E. *Annu. Rev. Phys. Chem.* **1990**, *41*, 477−496.

(5) Querner, C.; Reiss, P.; Bleuse, J.; Pron, A. *J. Am. Chem. Soc.* **2004**, *126* (37), 11574−11582.

10.1021/cm061105p CCC: $33.50
Published on Web 08/29/2006

class of hybrid materials with a high potential for applications in thin film solar cells. Polythiophenes have drawn significant research interest since the discovery of their solution processibility.[6] The synthesis of the title compounds consists of three steps: first, the coupling of a prefunctionalized thiophene monomer with oligothiophenes; second, the oxidative polymerization of the resulting symmetric oligomers yielding structurally well-defined polymers; and third, the introduction of the carbodithioate anchor function via a postfunctionalization reaction. This strategy gives the possibility of preparing a large variety of functional polythiophenes depending on the chemical structure of the oligothiophene building blocks used in the first step. Finally, the synthesis and optical properties of CdSe nanocrystals functionalized with the simplest compound of this family of molecules, that is, 4-thiophen-3-yldithiobenzoic acid, are described.

Experimental Section

Chemicals. All reagents and solvents were purchased from Aldrich or Acros in the highest purity available and used as received.

Characterization Methods. All synthesized products were identified by ^{1}H and ^{13}C NMR spectroscopy, as well as by elemental analysis. NMR spectra were recorded on a Bruker AC200 spectrometer. Acetone-d_6, chloroform-*d*, or dimethyl sulfoxide-d_6, containing tetramethylsilane as internal standard, was used as the solvent, depending on the solubility of the products. Elemental analyses (C, H, N, and S) were carried out by the Analytical Service of the CNRS in Vernaison, France. Ultraviolet−visible (UV−vis) absorption spectra were recorded on a HP 8452A spectrometer (wavelength range 190−820 nm). Solution phase photoluminescence (PL) measurements were carried out on an AvaSpec-2048-2 spectrofluorometer with a blue (400 nm) diode for excitation.

The molecular weights of the polymer fractions were determined by size-exclusion chromatography (SEC) on a 1100HP Chemstation equipped with a 300 × .5 mm^2 PL gel mixed-D 5 μm/10^4 Å column. Detection was performed by a diode array UV−vis detector and a refractive index detector. The column temperature and the flow rate were fixed to 313 K and 1 mL·min^{-1}, respectively. The calibration curve was built from 10 polystyrene (PS) narrow standards (S-M-10* kit from Polymer Labs). All molecular weights are given in equivalents of PS (equiv. PS). Polymer (20 μL of ca. 2 mg·mL^{-1} solution) in HPLC-grade tetrahydrofuran (THF) was injected and analyzed by UV−vis detection at 355 nm.

Cyclic voltammetry experiments were performed in a drybox filled with argon, by use of a one-compartment electrolytic cell with a platinum disk working electrode (7 mm^2 surface area), a platinum counter electrode, an Ag/0.1 M $AgNO_3$ reference electrode, and as the electrolyte a 0.1 M Bu_4NBF_4 solution in anhydrous dichloromethane, containing ∼10^{-3} M of the investigated molecules.

Nanocrystal Synthesis. The used nanocrystal samples were 3.2 nm in diameter (determined by TEM measurements) and have been prepared according to the procedure reported elsewhere.[7] UV−vis ($CHCl_3$) λ_{abs} (excitonic peak) = 546 nm; PL ($CHCl_3$) λ_{em} = 559 nm.

3-[4-(Bromomethyl)phenyl]thiophene (1). 3-Thienylboronic acid (2.53 g, 0.02 mol) was protected with 6.18 g (0.059 mol) of 2,2-dimethyl-1,3-propanediol in 100 mL of THF. The mixture was stirred for 1 h at room temperature and concentrated. The obtained crude product was dissolved in diethyl ether and washed several times with water. The organic phase was then dried over $MgSO_4$ and concentrated to yield 3.58 g (92%) of the corresponding boronic ester 5,5-dimethyl-2-(thien-3-yl)[1,3,2]dioxaborinane as a white solid. ^{1}H NMR (acetone-d_6, 200 MHz) δ 7.86 (1H, dd, J_1 = 2.7 Hz, J_2 = 1.1 Hz), 7.41 (1H, dd, J_1 = 4.8 Hz, J_2 = 2.7 Hz), 7.33 (1H, dd, J_1 = 4.8 Hz, J_2 = 1.1 Hz), 3.76 (4H, s), 1.00 (6H, s); ^{13}C NMR (acetone-d_6, 200 MHz) δ 22.9 (2C), 32.3, 73.7 (2C), 126.7, 133.5, 136.5, quaternary $C_{thiophene}B$ not visible. Anal. Calcd for $C_9H_{13}BO_2S$: C, 55.13; H, 6.68; B, 5.51; O, 16.32; S, 16.35. Found: C, 55.14; H, 6.62; S, 16.30.

5,5-Dimethyl-2-(thien-3-yl)[1,3,2]dioxaborinane (3.55 g, 18 mmol) and 3.05 g (16 mmol) of *p*-bromobenzaldehyde were coupled via a Suzuki reaction,[8] using 3.84 g (18 mmol) of K_3PO_4 and 0.95 g (0.8 mmol) of $Pd(PPh_3)_4$ in 60 mL of *N*,*N*-dimethylformamide (DMF) under argon flow. The mixture was heated at 110 °C for 15 h. After the mixture was cooled to room temperature, K_3PO_4 was removed by filtration and washed with diethyl ether. The filtrate was extracted with brine and washed with water. The organic phase was dried over $MgSO_4$ and concentrated. The crude product was purified by recrystallization in methanol to yield 2.24 g (72%) of 4′-thien-3-ylbenzaldehyde as a yellow solid. ^{1}H NMR ($CDCl_3$, 200 MHz) δ 9.94 (1H, s), 7.84 (2H, d, J = 8.6 Hz), 7.68 (2H, d, J = 8.4 Hz), 7.53 (1H, t, J = 2.2 Hz), 7.37 (2H, d, J = 2.4 Hz); ^{13}C NMR ($CDCl_3$, 200 MHz) δ 122.5, 126.1, 126.7 (2C), 126.9, 130.4 (2C), 135.0, 140.9 (2C), 191.7. Anal. Calcd for $C_{11}H_8OS$: C, 70.18; H, 4.28; O, 8.50; S, 17.03. Found: C, 70.02; H, 4.35; S, 16.07.

4′-Thien-3-ylbenzaldehyde (2.24 g, 12 mmol) was dissolved in anhydrous THF, placed under argon atmosphere, and cooled to 0 °C. Then 0.45 g (12 mmol) of sodium borohydride was added in small fractions.[9] The mixture was allowed to warm to room temperature and stirred overnight. Finally, water was added and the mixture was extracted with diethyl ether. The organic phase was dried over $MgSO_4$ and concentrated to yield 1.85 g (82%) of (4′-thien-3-ylphenyl)methanol, as a slightly beige solid. ^{1}H NMR (acetone-d_6, 200 MHz) δ 7.71 (1H, dd, J_1 = 2.6 Hz, J_2 = 1.5 Hz), 7.67 (2H, dt, J_1 = 8.5 Hz, J_2 = 1.7 Hz), 7.58−7.50 (2H, m), 7.40 (2H, d, J = 8.8 Hz), 4.65 (2H, s), 2.86 (1H, s); ^{13}C NMR (acetone-d_6, 200 MHz) δ 65.4, 121.9, 127.9 (2C), 128.0, 128.2, 128.9 (2C), 136.3, 143.4 (2C). Anal. Calcd for $C_{11}H_{10}OS$: C, 69.44; H, 5.30; O, 8.41; S, 16.85. Found: C, 69.42; H, 5.39; S, 17.60.

Subsequently, 1.85 g (10 mmol) of (4′-thien-3-ylphenyl)methanol and 3.84 g (15 mmol) of triphenylphosphine were placed in 60 mL of anhydrous THF, and then 2.61 g (15 mmol) of *N*-bromosuccinimide dissolved in 20 mL of anhydrous THF was added dropwise.[10] The mixture was stirred for 4 h at room temperature and then concentrated. The crude product was purified by column chromatography with diethyl ether (5%)/pentane (95%) as eluent, yielding 2.2 g (89%) of **1** as a white solid. ^{1}H NMR ($CDCl_3$, 200 MHz) δ 7.50 (2H, dt, J_1 = 8.3 Hz, J_2 = 1.9 Hz), 7.39 (1H, dd, J_1 = 2.4 Hz, J_2 = 1.6 Hz), 7.38−7.30 (4H, m), 4.46 (2H, s); ^{13}C NMR ($CDCl_3$, 200 MHz) δ 33.4, 120.7, 126.3, 126.8 (2C), 129.1, 129.5 (2C), 136.0 (2C), 141.6. Anal. Calcd for $C_{11}H_9BrS$: C, 52.19; H, 3.58; Br, 31.56; S, 12.67. Found: C, 52.71; H, 3.67; S, 13.04.

3-[4-(Bromomethyl)phenyl]-2,5-dibromothiophene (2). Compound **1** (4.0 g, 15.8 mmol) was placed in 60 mL of DMF at room temperature. Then, 7.0 g (39.4 mmol) of *N*-bromosuccinimide

(6) Jen, K. Y.; Miller, G. G.; Elsenbaumer, R. L. *J. Chem. Soc. Chem. Commun.* **1986**, 1346−1347.
(7) Reiss, P.; Bleuse, J.; Pron, A. *Nano Lett.* **2002**, *2* (7), 781−784.
(8) Suzuki, A. *Pure Appl. Chem.* **1991**, *63* (3), 419−422.
(9) Sellner, H.; Rheiner, P. B.; Seebach D. *Helv. Chim. Acta* **2000**, *85* (1), 352−387.
(10) Brenna, E.; Fuganti, C.; Grasselli, P.; Serra, S.; Zambotti, S. *Chem. Eur. J.* **2002**, *8* (8), 1872−1878.

(NBS) dissolved in 40 mL of DMF was added dropwise, and the reaction mixture was stirred overnight.[11] It was poured on ice for hydrolysis and then extracted by diethyl ether. The organic phase was dried over $MgSO_4$, concentrated, and purified by column chromatography with diethyl ether (10%)/pentane (90%) as eluent to yield 2.9 g (45%) of **2**, as a yellow solid. ^{1}H NMR ($CDCl_3$, 200 MHz) δ 7.39 (4H, s), 6.93 (1H, s), 4.45 (2H, s); ^{13}C NMR ($CDCl_3$, 200 MHz) δ 32.9, 108.0, 111.4, 128.7 (2C), 129.1 (2C), 131.5, 134.1, 137.5, 141.3. Anal. Calcd for $C_{11}H_7Br_3S$: C, 32.15; H, 1.72; Br, 58.33; S, 7.80. Found: C, 32.08; H, 1.76; Br, 58.20; S, 7.71.

5,5-Dimethyl-2-(3-octylthien-2-yl)[1,3,2]dioxaborinane (3). Compound **3** was prepared according to the procedure described in ref 12. Briefly, 5.0 g (25 mmol) of 3-*n*-octylthiophene were brominated with 4.76 g (27 mmol) of NBS in DMF. The crude product was purified by column chromatography with pentane as eluent to yield 6.29 g (90%) of 2-bromo-3-octylthiophene as a colorless liquid. ^{1}H NMR (acetone-d_6, 200 MHz) δ 7.44 (1H, d, J = 5.6 Hz), 6.93 (1H, d, J = 5.6 Hz), 2.58 (2H, t, J = 7.2 Hz), 1.59 (2H, q, J = 7.2 Hz), 1.25−1.10 (10H, m), 0,88 (3H, t, J = 6.7 Hz); ^{13}C NMR (acetone-d_6, 200 MHz) δ 15.3, 24.3, 30.8, 30.9, 31.0, 31.1, 31.4, 33.6, 109.8, 127.8, 130.4, 143.9. Anal. Calcd for $C_{12}H_{19}BrS$: C, 52.36; H, 6.96; Br, 29.03; S, 11.65. Found: C, 52.23; H, 6.87; Br, 28.85; S, 11.43.

2-Bromo-3-*n*-octylthiophene (7.73 g, 28 mmol) in anhydrous THF was added dropwise to 0.75 g (31 mmol) of dried magnesium turnings, and the mixture was refluxed for 1 h. The Grignard compound was then added to a solution of 22.7 mL (84 mmol) of tributylborate in THF at −78 °C and allowed to slowly warm to room temperature. The mixture was then hydrolyzed by diluted hydrochloric acid and extracted by diethyl ether. The organic phase was washed with water and dried over $MgSO_4$ for at least 1 h by adding 14.5 g (0.14 mol) of 2,2-dimethyl-1,3-propanediol. After filtration and concentration, the crude product was purified by column chromatography with diethyl ether (5%)/pentane (95%) as eluent, to yield 6.12 g (71%) of **3**, as a slightly yellow viscous liquid. ^{1}H NMR (acetone-d_6, 200 MHz) δ 7.52 (1H, d, J = 4.8 Hz), 7.01 (1H, d, J = 4.6 Hz), 3.78 (4H, s), 2.88 (2H, t, J = 7.8 Hz), 1.57 (2H, quint, J = 7.5 Hz), 1.4−1.2 (10H, m), 1.02 (6H, s), 0.9−0.8 (3H, m); ^{13}C NMR (acetone-d_6, 200 MHz) δ 15.3, 22.9 (2C), 24.3, 31.0, 31.1, 31.2, 32.4, 33.3, 33.5, 33.6, 73.7 (2C), 132.0, 132.3, 154.7. Anal. Calcd for $C_{17}H_{29}BO_2S$: C, 66.23; H, 9.48; B, 3.51; O, 10.38; S, 10.40. Found: C, 66.97; H, 9.85.

5-Bromo-3,3″-dioctyl-2,2′:5′,2″-terthiophene (4). Bis(thien-2,5-yl)boronic acid (3.82 g, 22 mmol) was transformed into the corresponding boronic ester with 23.0 g (220 mmol) of 2,2-dimethyl-1,3-propanediol in 100 mL of THF (vide supra). Bis-2,5-(5′,5′-dimethyl-[1′,3′,2′]dioxaborolan-2′-yl)thiophene (4.6 g, 67%) was obtained as a white solid. ^{1}H NMR ($CDCl_3$, 200 MHz) δ 7.58 (2H, s), 3.75 (8H, s), 1.01 (12H, s). Anal. Calcd for $C_{14}H_{22}B_2O_4S$: C, 54.59; H, 7.20; B, 7.02; O, 20.78; S, 10.41. Found: C, 54.37; H, 7.15; S, 10.27.

2,5-Bis(5′,5′-dimethyl[1′,3′,2′]dioxaborin-2′-yl)thiophene (4.6 g, 19.3 mmol) and 9.65 g (35.1 mmol) of 2-bromo-3-*n*-octylthiophene were coupled in a Suzuki reaction by use of 8.43 g (38.6 mmol) of K_3PO_4 and 2.23 g (2.0 mmol) of $Pd(PPh_3)_4$ in DMF, similarly to the above-described protocol for the preparation of 4′-thien-3-ylbenzaldehyde. The crude product was purified by column chromatography with pentane as eluent to yield 0.96 g (11%) of 3,3″-dioctyl-2,2′:5′,2″-terthiophene as a slightly yellow oil. ^{1}H NMR ($CDCl_3$, 200 MHz) δ 7.22 (2H, d, J = 5.2 Hz), 7.12 (2H, d, J = 3.8 Hz), 6.99 (2H, d, J = 5.2 Hz), 2.80 (4H, t, J = 7.6 Hz), 1.69 (4H, quint, J = 7.3 Hz), 1.4−1.2 (20H, m), 0.94 (6H, t, J = 7.0 Hz); ^{13}C NMR ($CDCl_3$, 200 MHz) δ 14.1, 22.6, 29.1, 29.2, 29.4, 29.5, 30.7, 31.9, 123.7, 125.9, 129.9, 136.2, 139.6, 142.0. Anal. Calcd for $C_{28}H_{40}S_3$: C, 71.13; H, 8.53; S, 20.35. Found: C, 71.07; H, 8.46; S, 20.16.

Finally, 0.47 g (1.0 mmol) of 3,3″-dioctyl-2,2′:5′,2″-terthiophene was monobrominated with 0.18 g (1.0 mmol) of NBS (vide supra). The crude product was purified by column chromatography with pentane as eluent to yield 0.41 g (74%) of **4** as a viscous yellow liquid. ^{1}H NMR ($CDCl_3$, 200 MHz) δ 7.15 (1H, d, J = 5.1 Hz), 7.05 (1H, s), 6.98 (1H, d, J = 3.8 Hz), 6.90 (1H, d, J = 5.1 Hz), 6.82 (1H, d, J = 3.8 Hz), 2.67 (4H, quint, J = 8.2 Hz), 1.58 (4H, quint, J = 7.6 Hz), 1.4−1.2 (20H, m), 0.85 (6H, t J = 6.4 Hz); ^{13}C NMR ($CDCl_3$, 200 MHz) δ 14.0 (2C), 23.1 (2C), 23.7, 24.4, 30.0 (4C), 30.4 (2C), 32.5 (2C), 33.4 (2C), 113.8, 123.6 (2C), 125.8, 130.2, 133.6, 133.9, 135.1, 138.3, 140.9, 142.3 (2C). Anal. Calcd for $C_{28}H_{39}BrS_3$: C, 60.96; H, 7.13; Br, 14.48; S, 17.44. Found: C, 60.69; H, 7.01; Br, 14.00; S, 16.89.

3′-[4-(Bromomethyl)phenyl]-3,3″-dioctyl[2,2′:5′,2″]terthiophene (5). Compound **2** (1.23 g, 3 mmol) and 2.03 g (6.6 mmol) of **3** were placed in 40 mL of DMF, and 1.40 g (6.6 mmol) of K_3PO_4 as well as 0.35 g (0.3 mmol) of $Pd(PPh_3)_4$ were added. The procedure and workup for this Suzuki reaction were identical to the ones used for the preparation of **4**. The crude product was purified by column chromatography with pentane as eluent to yield 1.0 g (53%) of **5** as a viscous yellow liquid. ^{1}H NMR ($CDCl_3$, 200 MHz) δ 7.33 (2H, d, J = 8.2 Hz), 7.20 (2H, d, J = 8.2 Hz), 7.00 (1H, s), 7.05 (2H, d, J = 5.1 Hz), 6.87 (2H, d, J = 5.1 Hz), 4.05 (2H, s), 2.45 (4H, t, J = 7.4 Hz), 1.55 (4H, quint, J = 6.8 Hz), 1.4−1.1 (20H, m), 0.80 (6H, t, J = 6.8 Hz); ^{13}C NMR ($CDCl_3$, 200 MHz) δ 14.0 (2C), 23.1 (2C), 24.4 (2C), 29.9 (4C), 30.3 (2C), 32.5 (3C), 33.4 (2C), 121.3, 125.8 (2C), 127.3 (2C), 129.7 (2C), 130.2 (2C), 133.6 (2C), 136.6, 138.0, 138.5 (3C), 139.2, 144.9. Anal. Calcd for $C_{35}H_{45}BrS_3$: C, 65.50; H, 7.07; Br, 12.45; S, 14.99. Found: C, 65.25; H, 7.00; Br, 12.22; S, 14.63.

3‴-[4-(Bromomethyl)phenyl]-3,3″,4⁗,3⁗⁗⁗-tetraoctyl[2,2′:5′,2″:5″,2‴:5‴,2⁗:5⁗,2⁗⁗⁗:5⁗⁗⁗,2⁗⁗⁗⁗⁗]septithiophene (6). Compound **4** (550 mg, 1 mmol) was placed in 50 mL of anhydrous THF under argon atmosphere, and 0.5 mL (1 mmol) of a 2 M ClMg-*t*Bu solution in diethyl ether was added. This reaction mixture was refluxed for 1 h. Then, 205 mg (0.5 mmol) of **2** dissolved in 5 mL of THF and 27 mg (0.05 mmol) of $Ni(dppp)Cl_2$ were added, and the reaction was maintained under reflux for an additional hour.[13] The workup was similar to the one used in the Suzuki reactions described above, including hydrolysis by water, extraction by diethyl ether, drying of the organic phase over $MgSO_4$, and purification of the crude product by column chromatography with diethyl ether (5%)/pentane (95%) as eluent, to yield 0.55 g (91%) of **6** as a yellow-orange, viscous liquid. ^{1}H NMR ($CDCl_3$, 200 MHz) δ 7.4−7.3 (2H, m), 7.2−6.9 (9H, m), 6.8−6.6 (4H, m), 4.06 (2H, s), 2.6−2.4 (8H, m), 1.6−1.5 (8H, m), 1.4−1.1 (40H, m), 0.9−0.8 (12H, m); ^{13}C NMR ($CDCl_3$, 200 MHz) δ 14.1 (4C), 23.0 (4C), 24.5 (4C), 30.0 (12C, m), 32.5 (9C, m), 121.8, 123.5 (4C), 126.0 (4C), 127.1 (2C), 130.0 (4C), 133.9 (4C), 136.7, 138.2 (6C), 139.2, 143.0 (6C), 144.5. Anal. Calcd for $C_{67}H_{85}BrS_7$: C, 67.35; H, 7.15; Br, 6.69; S, 18.79. Found: C, 66.78; H, 6.99; Br, 7.01; S, 17.97.

General Polymerization Procedure.[14] The monomer (1 equiv) was dissolved in anhydrous chloroform and placed under argon

(11) Bäuerle, P.; Pfau, F.; Schlupp, H.; Würthner, F.; Gaudl, K. U.; Balparda Caro, M.; Fischer, P. *J. Chem. Soc., Perkin Trans. 2* **1993**, 489−494.

(12) (a) Bidan, G.; De Nicola, A.; Enée, V.; Guillerez, S. *Chem. Mater.* **1998**, *10* (4), 1052−1058. (b) Demadrille, R.; Divisia-Blohorn, B.; Zagorska, M.; Quillard, S.; Lefrant, S.; Pron, A. *Electrochim. Acta* **2005**, *50* (7−8), 1597−1603.

(13) (a) Loewe, R. S.; Ewbank, P. C.; Liu, J.; Zhai, L.; McCullough, R. *Macromolecules* **2001**, *34* (13), 4324−4333. (b) Katz, H. E.; Bao, Z.; Gilat, S. L. *Acc. Chem. Res.* **2001**, *34* (5), 359−369.

atmosphere at 0 °C. Anhydrous $FeCl_3$ (3 equiv) was dissolved in a mixture of anhydrous chloroform (75%) and anhydrous nitromethane (25%). The oxidant solution was then slowly added to the monomer solution. After 1 h, the cooling bath was removed and the reaction was continued at room temperature. Finally, the polymer was precipitated in methanol, filtered, and washed. Then, it was dispersed in 0.1 M NH_4OH for at least 1 h and filtered. This dedoping step was repeated twice for 24 h. The polymer was then dispersed in a 0.1 M EDTA solution and finally in water. After filtration, it was dried under vacuum until the mass remained constant.

Poly(3′-[4-(Bromomethyl)phenyl]-3,3″-dioctyl[2,2′:5′,2″]terthiophene-5,5″-diyl) (7). $FeCl_3$ (724 mg, 4.46 mmol) in 15 mL of $CHCl_3$ and 5 mL of CH_3NO_2 was added to a solution of 715 mg (1.12 mmol) of monomer **5** in 15 mL of anhydrous $CHCl_3$. The total polymerization time was 3 h. The reaction mixture was then poured into 400 mL of methanol and the workup was performed according to the general polymerization procedure to yield 0.66 g (92%) of the orange-red polymer **7**. The polymer (554 mg) was then fractionated by Soxhlet extraction with the following solvent sequence[15] (the values in parentheses correspond to quantity of the obtained polymer fraction): methanol (40 mg), diethyl ether (150 mg), acetone (10 mg), pentane (6 mg), dichloromethane (10 mg), THF (66 mg), and chloroform (22 mg). A total of 190 mg was recovered as chloroform-nonsoluble fraction. ^{1}H NMR (batch, $CDCl_3$, 200 MHz) δ 7.35 (2H, s), 7.18 (2H, s), 6.98 (1H, s), 6.57 (2H, s), 4.09 (2H, s), 2.48 (4H, br s), 1.61 (4H, br s), 1.22 (20H, br s), 0.82 (6H, br s). UV−vis ether fraction ($CHCl_3$) λ_{max} = 406 nm ($\pi-\pi^*$); PL ($CHCl_3$) λ_{em} = 556 nm.

Poly(3‴-[4-(Bromomethyl)phenyl]-3,3″,4⁗,3⁗′′-tetraoctyl-[2,2′:5′,2″:5″,2‴:5‴,2⁗:5⁗,2⁗′:5⁗′,2⁗′′:5⁗′′,2⁗′′′]septithiophene-5,5⁗′′′-diyl) (8). Monomer **6** (190 mg, 0.16 mmol) was polymerized for 5 h with 111 mg (0.68 mmol) of $FeCl_3$ to yield, after an identical workup as described before, 100 mg (53%) of the dark-red polymer **8**. ^{1}H NMR ($CDCl_3$, 200 MHz) δ 7.33 (2H, br s), 7.2−6.8 (7H, m), 6.67 (4H, br s), 4.12 (2H, s), 2.51 (8H, br s), 1.58 (8H, br s), 1.25 (40H, br s), 0.82 (12H, br s). UV−vis ($CHCl_3$) λ_{max} = 436 nm ($\pi-\pi^*$); PL ($CHCl_3$) λ_{em} = 560 nm.

General Procedure for the Introduction of the Carbodithioate Function.[16] Elemental sulfur (2 equiv) and 2 equiv of sodium methanolate (NaOMe) were placed in anhydrous methanol under argon atmosphere and refluxed until the sulfur was completely dissolved (ca. 2 h). Then, 1 equiv of the arylmethylene bromide compound (**1**, **7**, or **8**) was added in the solid form to the reaction mixture, which was refluxed overnight. The solvent was evaporated and the obtained red solid was dissolved in water. Acidification with diluted HCl led to the precipitation of the carbodithioic acid, which was filtered under argon atmosphere and washed several times with water. The product was dissolved in dichloromethane, dried over $MgSO_4$, and concentrated.

4-Thiophen-3-yldithiobenzoic acid (9). To a solution of 0.19 g (6 mmol) of S and 0.32 g (6 mmol) of NaOMe in methanol, which had been refluxed for 2 h, was added 0.76 g (3 mmol) of **1**, and the mixture was refluxed for an additional 15 h. The workup according to the general procedure yielded 0.66 g (93%) of **9** as a dark-red solid. ^{1}H NMR ($CDCl_3$, 200 MHz) δ 8.04 (2H, dt, J_1 = 8.8 Hz, J_2 = 2.2 Hz), 7.54 (3H, dt+d, J_1 = 8.8 Hz, J_2 = 2.2 Hz, J_3 = 2.0 Hz), 7.36 (2H, d, J = 2.2 Hz), 6.21 (1H, s); ^{13}C NMR ($CDCl_3$, 200 MHz) δ 122.3, 126.1 (2C), 126.9 (2C), 127.7 (2C), 128.8, 140.5, 140.8, 141.7, 223.6. Anal. Calcd for $C_{11}H_8S_3$: C, 55.89; H, 3.41; S, 40.69. Found: C, 55.38; H, 3.42; S, 39.58. UV−vis ($CHCl_3$) λ_{max} = 358 nm ($\pi-\pi^*$); PL ($CHCl_3$) λ_{em} = 460 nm.

Poly(3′-[4-(dithiocarboxy)phenyl]-3,3″-dioctyl[2,2′:5′,2″]terthiophene-5,5″-diyl) (10). To a solution of 15 mg (0.47 mmol) of S and 25.4 mg (0.47 mmol) of NaOMe in methanol, refluxed for 2 h, was added 150 mg (0.23 mmol) of the ether fraction of the polymer **7**, and the mixture was refluxed for an additional 15 h. The workup was carried out according to the general procedure to yield 120 mg (84%) of the functionalized polymer **10** as a dark red-brown solid. ^{1}H NMR ($CDCl_3$, 200 MHz) δ 8.02 (2H, br s), 7.49 (2H, br s), 7.02 (1H, br s), 6.65 (2H, br s), 2.52 (4H, br s), 1.64 (4H, br s), 1.23 (20H, br s), 0.85 (6H, br s); ^{13}C NMR ($CDCl_3$, 200 MHz) δ 225.7 (-CS_2H). Anal. Calcd for $C_{35}H_{42}S_5$: C, 67.47; H, 6.79; S, 25.73. Found: C, 67.08; H, 6.85; S, 24.15. UV−vis ($CHCl_3$) λ_{max} = 414 nm ($\pi-\pi^*$); PL ($CHCl_3$) λ_{em} = 558 nm.

Poly(3‴-[4-(dithiocarboxy)phenyl]-3,3″,4⁗,3⁗′′-tetraoctyl-[2,2′:5′,2″:5″,2‴:5‴,2⁗:5⁗,2⁗′:5⁗′, 2⁗′′:5⁗′′,2⁗′′′]septithiophene-5,5⁗′′′-diyl) (11). To a solution of 1.6 mg (0.05 mmol) of S and 2.7 mg (0.05 mmol) of NaOMe in methanol, refluxed for 2 h, was added 27.6 mg (0.025 mmol) of the polymer **8**, and the mixture was refluxed for an additional 15 h. The workup was carried out according to the general procedure to yield 20 mg (68%) of the functionalized polymer **11** as a dark red-brown solid. ^{1}H NMR ($CDCl_3$, 200 MHz) δ 7.98 (2H, br s), 7.39 (2H, br s), 7.2−6.8 (7H, m), 6.67 (4H, br s), 2.51 (8H, br s), 1.58 (8H, br s), 1.25 (40H, br s), 0.82 (12H, br s); ^{13}C NMR ($CDCl_3$, 200 MHz) δ 224.9 (-CS_2H). Anal. Calcd for $C_{67}H_{82}S_9$: C, 68.43; H, 7.03; S, 24.54. Found: C, 69.03; H, 7.32; S, 22.01. UV−vis ($CHCl_3$) λ_{max} = 434 nm ($\pi-\pi^*$); PL ($CHCl_3$) λ_{em} = 559 nm.

General Procedure for Grafting of Carbodithioic Acids on the Surface of Nanocrystals.[5] A solution of nanocrystals in chloroform was mixed with a solution of the carbodithioic acid in the same solvent. The latter was used in a 2−5-fold excess with respect to the cadmium sites on the surface of the nanoparticles estimated from their size. The mixture was stirred for 1−2 h and precipitated with methanol. For the purification of the hybrids, washing with a sequence of solvents was then applied to remove excess ligands.

CdSe-9. Compound **9** (60 mg) in 10 mL of $CHCl_3$ was added to 30 mg of CdSe nanocrystals (diameter = 3.2 nm) in 5 mL of $CHCl_3$, and the mixture was stirred for 2 h and precipitated with methanol. The dark-red hybrid was washed with methanol, diethyl ether, and chloroform to remove excess ligands. ^{1}H NMR (DMSO-d_6, 200 MHz) δ 8.29 (2H, br d, $J \sim$ 8 Hz), 8.02 (1H, dd, J_1 = 2.8 Hz, J_2 = 1.4 Hz), 7.75 (2H, d, J = 8.6 Hz), 7.7−7.6 (2H, m). UV−vis (DMSO) λ_{max} = 358 nm ($\pi-\pi^*$).

Results and Discussion

Synthesis of Carbodithioate-Functionalized Oligo- and Polythiophenes. We chose a sequential synthesis (Scheme 1) via 3-[4-(bromomethyl)phenyl]-2,5-dibromothiophene (**2**), that is, a prefunctionalized precursor, for the preparation of the title compounds. Using this molecule brings several advantages. It serves as a central building block allowing for the synthesis of polymerizable monomers. As there are two aromatic bromine atoms and one aliphatic one, the coupling of oligothiophenes, for example, via Suzuki or Kumada coupling, should preferentially occur in the α-positions of the thiophene rings, preserving the arylmethylene bromine group. Depending on the oligothiophene building

(14) Andersson, M. R.; Selse, D.; Berggren, M.; Jaervinen, H.; Hjertberg, T.; Inganaes, O.; Wennerstroem, O.; Oesterholm, J. E. *Macromolecules* **1994**, *27* (22), 6503−6506.
(15) Trznadel, M.; Pron, A.; Zagorska, M.; Cszaszcz, R.; Pielichowski, J. *Macromolecules* **1998**, *31* (15), 5051−5058.
(16) (a) Bryce, M. R. *J. Chem. Soc., Perkin Trans. 1* **1985**, 1675−1679. (b) Fabre, J. M.; Torreilles, E.; Giral, L. *Tetrahedron Lett.* **1978**, *39*, 3703−3706.

Scheme 1. Synthetic Pathway for Carbodithioate-Functionalized Oligo- and Polythiophenes[a]

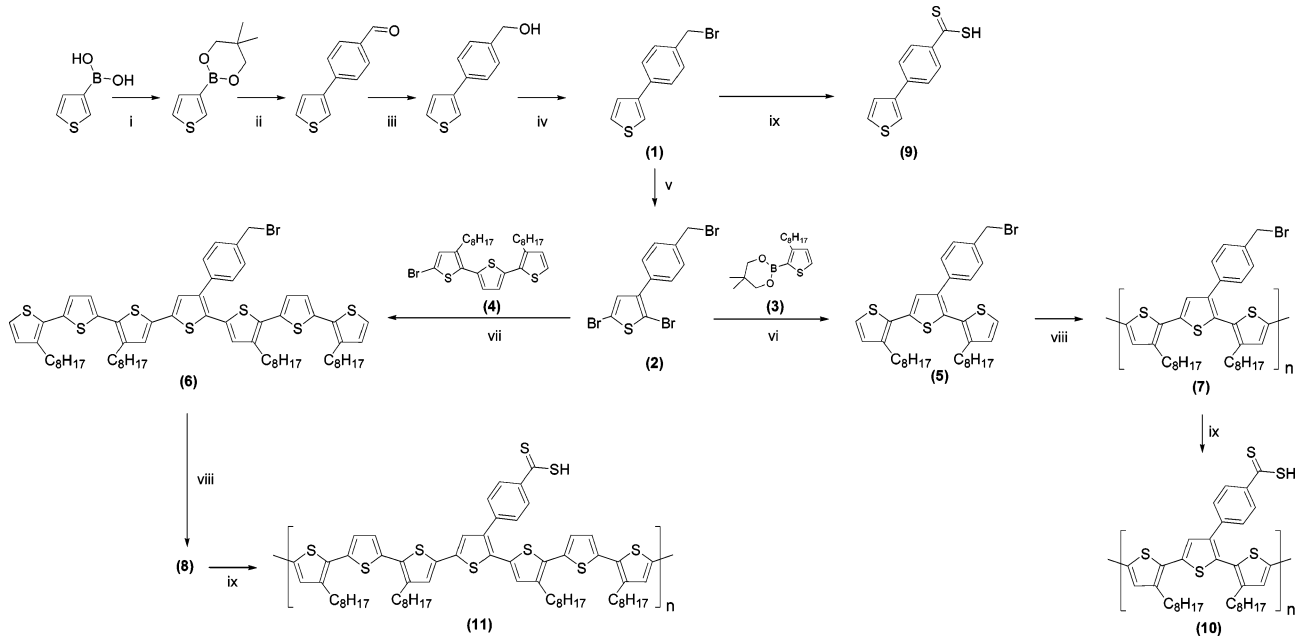

[a] Reagents and conditions: (i) HO-C_5H_{10}-OH, THF, 1 h, rt; $\eta = 92\%$; (ii) OHC-C_6H_5-Br, K_3PO_4, $Pd(PPh_3)_4$, DMF, 15 h, 110 °C, $\eta = 72\%$; (iii) $NaBH_4$, THF, 12 h, 0 °C, $\eta = 82\%$; (iv) PPh_3, NBS, THF, 4 h, rt, $\eta = 89\%$; (v) NBS, DMF, 12 h, rt, $\eta = 45\%$; (vi) **3**, K_3PO_4, $Pd(PPh_3)_4$, DMF, 15 h, 110 °C, $\eta = 53\%$; (vii) **4**, 2 M ClMg-*t*Bu, $Ni(dppp)Cl_2$, THF, 2 h, reflux, $\eta = 91\%$; (viii) $FeCl_3$, $CHCl_3$, 3 h, rt; (ix) S, NaOMe, MeOH, 15 h, reflux.

blocks used for the coupling, a large variety of quasisymmetric monomers can be obtained, which can be subsequently polymerized into regioregularly well-defined polymers.

During the preparation of carbodithioic acids, the CS_2 group is generally introduced in the last step because of its reactivity and sensitivity. We observed that the usually applied Grignard reaction involving carbon disulfide[17] does not yield a quantitative conversion of the bromine functions in the synthesized polythiophene derivatives. It can be achieved, however, when a mixture of elemental sulfur and sodium methanolate is used for the conversion reaction.[16]

Compound **2** has been synthesized in a five-step reaction with an overall yield of 25%, including the preparation of 4′-thien-3-ylbenzaldehyde, (4′-thien-3-ylphenyl)methanol, and 3-[4-(bromomethyl)phenyl]thiophene (**1**), followed by a dibromination reaction. The prepared intermediates (aldehyde and alcohol) are also interesting precursors for the preparation of functional monomers and polymers after mono- or dibromination of the α-positions of the thiophene ring. The oligothiophenes have been prepared by classical cross-coupling reactions, for example, of Suzuki type, according to literature procedures.[8,13,18] They are then coupled to compound **2** in good yields, leading to quasisymmetric functional oligomers.

These building blocks (terthiophene **5** and septithiophene **6**) have then been polymerized by chemical oxidation with $FeCl_3$.[14] As this method is known to yield relatively high molecular weight polymers in comparably short reaction

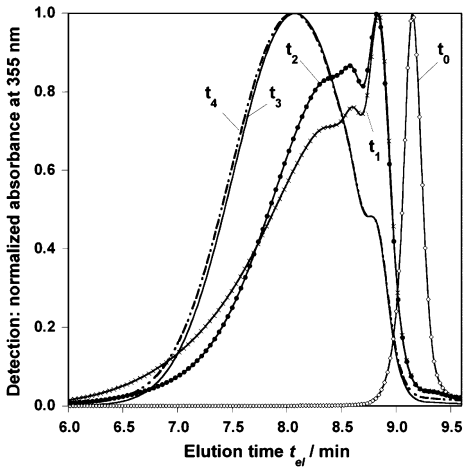

Figure 1. SEC elugrams of monomer **5** (t_0) and the corresponding polymer fractions **7** taken after different polymerization times ($t_1 = 1$ h, $t_2 = 2$ h, $t_3 = 3.5$ h, and $t_4 = 5$ h), recorded in THF.

times, we carried out a "screening polymerization" to study the evolution of molecular weight as a function of polymerization time. The solubility of the polymer, which depends on its molecular weight, is expected to decrease during the subsequent functionalization step and its grafting to nanocrystals. Therefore, it is of crucial importance to determine its appropriate molecular weight: it should be relatively high, to ensure good film-forming properties, but at the same time low enough to keep the obtained organic/inorganic hybrids soluble. Figure 1 compares the size-exclusion chromatograms of samples taken after different polymerization periods during the screening polymerization of **5** with the monomer (t_0). It is clearly visible that, after short polymerization times ($t_1 =$ 1 h), essentially dimers and some higher oligomers are formed. Further polymerization ($t_2 = 2$ h) increases the higher molecular weight oligomer fraction. Even longer polymerization times lead to partially insoluble polymers (~20 wt

(17) (a) Houben, J.; Pohl, H. *Ber. Dtsch. Chem. Ges.* **1907**, *40*, 1725−1731. (b) Colorado, R.; Villazana, R. J.; Lee, T. R. *Langmuir* **1998**, *14* (22), 6337−6340.

(18) (a) Guillerez, S.; Bidan, G. *Synth. Met.* **1998**, *93* (2), 123−126. (b) Stille, J. K. *Angew. Chem., Int. Ed. Engl.* **1986**, *25* (6), 508−523. (c) McCullough, R. D.; Lowe, R. D.; Jayaraman, M.; Anderson, D. L. *J. Org. Chem.* **1993**, *58* (4), 904−912.

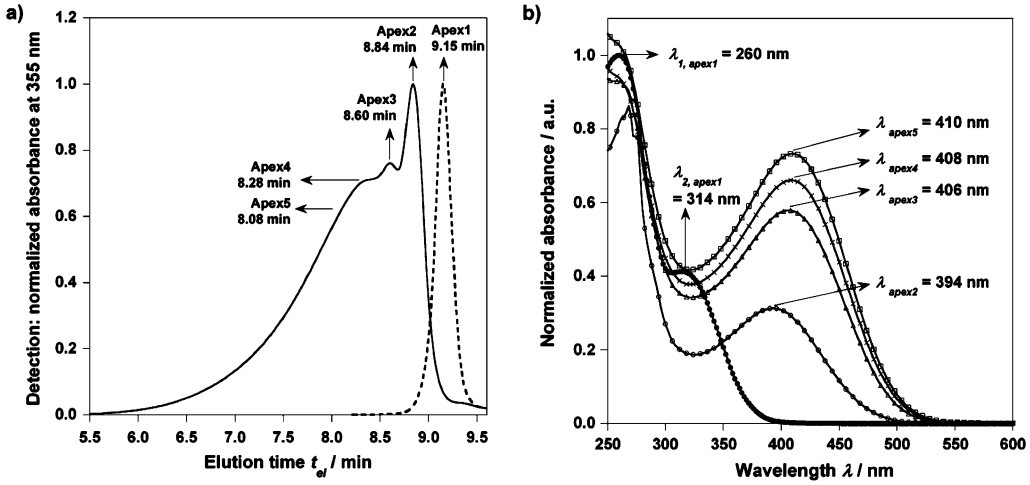

Figure 2. (a) SEC elugrams of monomer **5** (apex1) and the polymer fraction after 1 h of polymerization (t_1). (b) UV−visible absorption spectra recorded in situ at the indicated apexes, corresponding to dimer (apex 2), trimer (apex 3), tetramer (apex 4), and higher oligomers (apex 5).

% for $t_3 = 3.5$ h and ~50 wt % for $t_4 = 5$ h). The soluble parts of these two polymer fractions show almost identical elugrams, indicating that a solubility limit in THF has been reached and showing that all further polymerization would only lead to an increase of the insoluble fraction. They have a major composition of hexa- to octamers (determined from the value of M_p, i.e. the molecular weight at the apex of the peak), corresponding to 18 and 24 thiophene rings, respectively, and a rather low content in smaller oligomers.

Because of the rather high molecular weight of the monomer ($M = 641$ g·mol^{-1}), we can clearly distinguish between the small oligomers formed (dimer, trimer, tetramer, and minor contribution of higher oligomers). Figure 2a shows a more detailed analysis of the elugram of polymer **7** obtained after 1 h of polymerization, and Figure 2b represents the UV−visible absorption spectra, recorded in situ during the SEC analyses, corresponding to the different species present in the fraction. The red shift of the $\pi-\pi^*$ transition can clearly be observed as the oligomers get longer: from 394 nm in the dimer to 408 nm in the tetramer and to 410 nm in the case of higher oligomers.

By comparing the determined molecular weights from the peak positions M_p with the one calculated from the chemical formula M_{calc}, we observe an underestimation in the case of the dimer [$t_{el} = 8.84$ min, $M_p = 850$ g·mol^{-1} (equiv. PS), $M_{calc} = 1282$ g·mol^{-1}], whereas for the tetramer [$t_{el} = 8.28$ min, $M_p = 3640$ g·mol^{-1} (eq PS), $M_{calc} = 2561$ g·mol^{-1}] the molecular weight is overestimated by SEC. Indeed, molecular weights above 2000 g·mol^{-1} are systematically overestimated by SEC and the correction factor increases for increasing masses. This behavior has been described for poly(alkylthiophene)s[19] as well as for thiophene-based copolymers.[20] We can therefore conclude that also the molecular weights of the higher oligomer and polymer fractions are overestimated.

With the goal to get a larger fraction of soluble polyterthiophene, we increased the number of solubilizing alkylthiophene rings with respect to the number of anchor functions by using monomer **6**. The associated polymerization led, after 5 h of reaction time, to a completely soluble polymer with molecular weights reaching up to 90 kDa (equiv. PS), even though the oligomer fraction is still high.

The conversion of the methylene bromine groups in compounds **1**, **7**, and **8**, respectively, into carbodithioic acid functions is achieved by a reaction involving elemental sulfur and sodium methanolate, which are refluxed in methanol[16] in a first step to generate in situ the reactive species, which are very sensitive to oxygen. The thiophene compound is then directly added in its solid form (compound **1**, **7**, or **8)**, which results in higher reaction yields than in the case of the addition of viscous liquids, nonmiscible with methanol (compound **5** or **6**). Proton NMR spectroscopy exhibits a quantitative conversion of the bromine groups in the polymers. The characteristic peaks of the methylene group in the vicinity of bromine at ca. 4.1 ppm are no longer visible, whereas a broad peak arising from the proton in the carbodithioic acid function at 6.2 ppm can be observed. This group is also at the origin of a supplementary signal at 225 ppm in the ^{13}C NMR spectrum. Figure 3a shows the UV−visible absorption spectra of the poly(terthiophene) before and after postfunctionalization. The introduction of the carbodithioic acid function leads to a bathochromic shift of ca. 8 nm of the band associated with the $\pi-\pi^*$ transition, indicating an extension of the π-conjugated system including the acid group. As shown in Figure 3b, the photoluminescence properties remain essentially unchanged after the postfunctionalization step. An analogous evolution of the optical properties is observed in the case of poly(septithiophene) (compounds **8** and **11**).

Figure 4 shows the electrochemical response of thiophene-dithiobenzoic acid (**9**) for five subsequent cycles recorded in 0.1 M Bu_4NBF_4/CH_2Cl_2, revealing a reversible redox couple ($E_{ox} = 1.4$ V vs Ag/Ag$^+$, $E_{red} = 1.0$ V vs Ag/Ag$^+$). The oxidation peak overlaps with the increasing, irreversible oxidation peak associated with the polymerization of **9**, which induces the formation of a red deposit on the working electrode. The potentials of the redox couple are higher than in the case of alkyl- or arylthiophene-based systems[22] because of the electron-withdrawing nature of the carbodithioic acid,

(19) Liu, J.; Loewe, R. S.; McCullough, R. D. *Macromolecules* **1999**, *32* (18), 5777−5785.
(20) Demadrille, R.; Rannou, P.; Bleuse, J.; Oddou, J. L.; Pron, A. *Macromolecules* **2003**, *36* (19), 7045−7054.

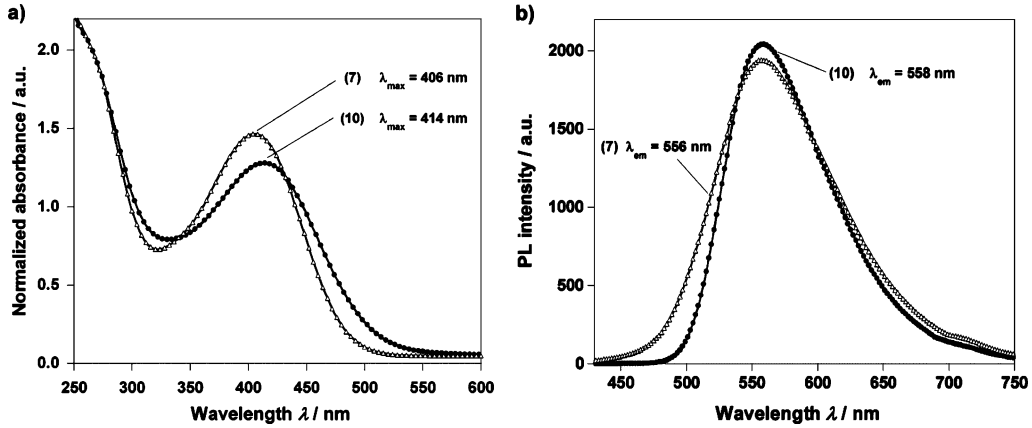

Figure 3. (a) UV−visible absorption spectra of poly(terthiophene) before (**7**) and after (**10**) introduction of the carbodithioic acid function, recorded in chloroform. (b) PL spectra of compounds **7** and **10**, by use of chloroform solutions of identical optical densities at the excitation wavelength (400 nm).

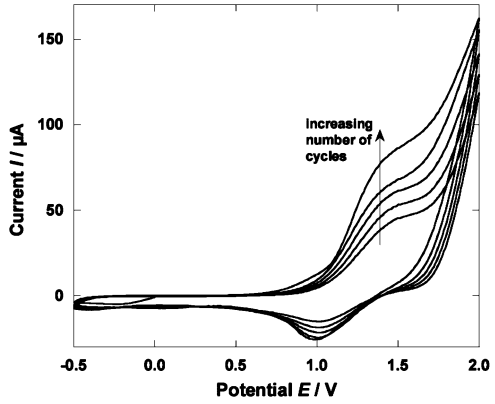

Figure 4. Cyclic voltammogram of **9**, recorded in 0.1 M Bu_4NBF_4 in CH_2Cl_2. Reference electrode Ag/0.1 M Ag^+; scan rate 100 mV/s.

which reduces the electron density of the α-positions in the thiophene ring. Therefore, the electron extraction in this position is more difficult and the polymerization occurs at higher potentials.

Figure 5a shows the cyclic voltammogram of polymer **7**, recorded in 0.1 M Bu_4NBF_4/CH_2Cl_2. The polymer adsorbed to the electrode during its oxidation to the radical cation and desorbed during its reduction ($E_{ox} = 0.69$ V vs Ag/Ag^+, $E_{red} = 0.57$ V vs Ag/Ag^+) without forming any deposit, which is consistent with the constant current intensity from one cycle to the following. The current intensity varies proportionally to the square root of the scan rate, indicating that diffusion processes dominate the reactions occurring at the electrode. During the cycling over a larger potential range, we observe an irreversible overoxidation peak ($E_{ox} = 1.8$ V vs Ag/Ag^+), as well as a cathodic peak ($E_{red} = -0.95$ V vs Ag/Ag^+). Overoxidation peaks are generally observed in electrochemical studies of oligo- or polythiophenes,[23] and they are usually located in the immediate vicinity of the doping peaks at higher potential values.

The cyclic voltammogram of **10**, represented in Figure 5b, is characterized by a reversible redox couple associated with the formation of the radical cation ($E_{ox} = 0.92$ V vs Ag/Ag^+, $E_{red} = 0.67$ V vs Ag/Ag^+), whose current intensity varies proportionally to the square root of the scan rate. Consistent with the previous measurements on compounds **7** and **9**, respectively, this redox couple is shifted to higher potential values due to the electron-withdrawing effect of the carbodithioate group. The poly(septithiophene)s, compounds **8** and **11**, exhibit very similar electrochemical behavior.

In addition to the presented fundamental characterization data of the prepared oligo- and polythiophenes, the electrochemical studies provide significant information on the position of their electronic energy levels. This knowledge is of particular interest if, after hybrid formation with semiconductor nanocrystals, their application in active layers of photovoltaic devices is aimed. In this type of application a staggered (type II) alignment of the oligo- or polythiophene highest occupied molecular orbital (HOMO) and lowest unoccupied molecular orbital (LUMO) levels and of the hole and electron state of the nanocrystals is required.[3e,f] Following the method described by Polec et al.,[24] the position of the HOMO of **10** and **11** with respect to the vacuum can be estimated from the electrochemically determined oxidation potential, whereas the size-dependent HOMO and LUMO levels of CdSe nanocrystals can be found in the literature.[25] Taking into account the optical band gap of polythiophene,[26] a staggered energy level alignment of **10** (**11**) and of CdSe nanocrystals can be postulated.

Functionalization of CdSe Nanocrystals with Thiophenedithiobenzoic Acid (9). We recently demonstrated that carbodithioates readily exchange ligands initially capping the surface of CdSe nanocrystals, such as TOPO or carboxylic acids, in short times at room temperature.[5] Functionalization with the newly synthesized oligo- and polythiophene derivatives can be carried out in exactly the same manner as illustrated in the following example. Thiophenedithiobenzoic acid (**9**) was grafted on the surface of CdSe nanocrystals by stirring both components for 2 h in chloroform. The obtained hybrid CdSe−**9** was purified by precipitation with methanol

(21) Furlani, C.; Luciani, M. L. *Inorg. Chem.* **1968**, *7*, 1586−1592.
(22) (a) Jing, F.; Tang, H.; Wang, C. *J. Solid State Electrochem.* **2004**, *8* (11), 877−881. (b) Hagenström, H.; Schneeweiss, M. A.; Kolb, D. M. *Langmuir* **1999**, *15* (22), 7802−7809.
(23) Krische, B.; Zagorska, M. *Synth. Met.* **1989**, *28* (1−2), 257−262.
(24) Polec, I.; Henckens, A.; Goris, L.; Nicolas, M.; Loi, M. A.; Adriaensens, P. J.; Lutsen, L.; Manca, J. V.; Vanderzande, D.; Sariciftci, N. S. J. *Polym. Sci. A: Polym. Chem.* **2003**, *41* (7), 1034−1045.
(25) Querner, C.; Reiss, P.; Sadki, S.; Zagorska, M.; Pron, A. *Phys. Chem. Chem. Phys.*, **2005**, *7* (17), 3204−3209.
(26) Sakurai, K.; Tachibana, H.; Shiga, N.; Terakura, C.; Matsumoto, M.; Tokura, Y. *Phys. Rev. B* **1997**, *56* (15), 9552−9556.

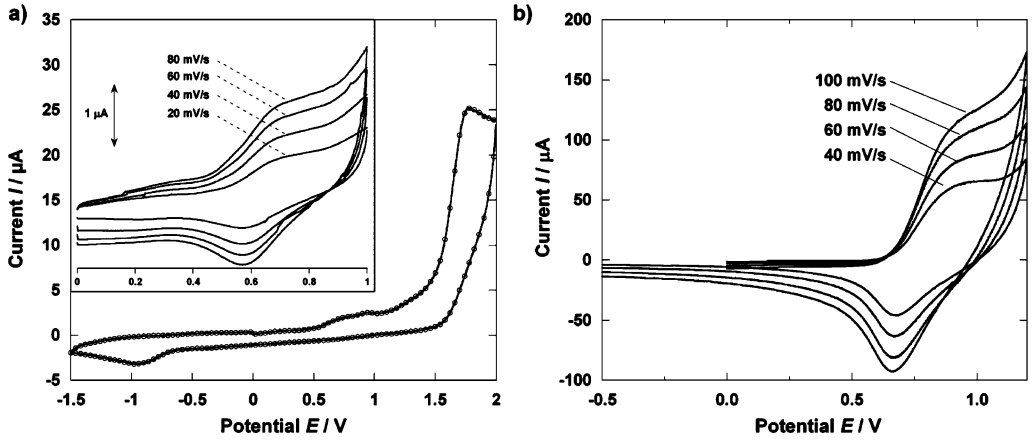

Figure 5. Cyclic voltammograms of (a) **7** and (b) **10** recorded in 0.1 M Bu_4NBF_4 in acetonitrile; reference electrode Ag/0.1 M Ag^+.

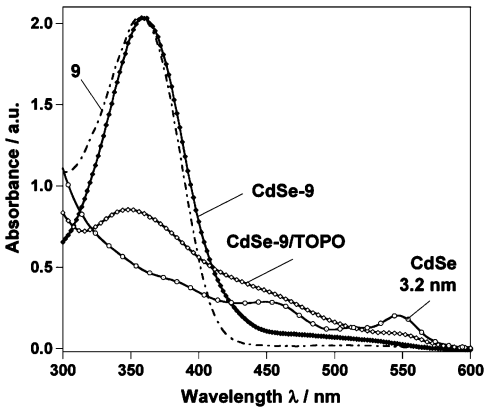

Figure 6. Solution UV−visible absorption spectra of TOPO-capped CdSe nanocrystals (diameter = 3.2 nm), of thiophenedithiobenzoic acid **9**, and of the corresponding hybrid compounds, after partial (CdSe−**9**/TOPO) and complete ligand exchange (CdSe−**9**), recorded in chloroform and DMSO, respectively.

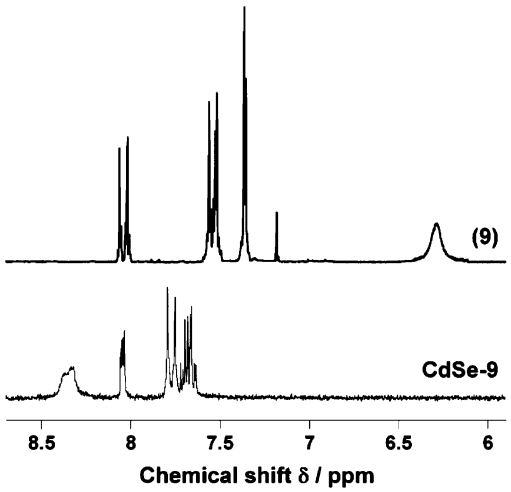

Figure 7. NMR spectra of **9**, recorded in $CDCl_3$, and of CdSe−**9**, recorded in DMSO-d_6.

to remove desorbed TOPO ligands, followed by the removal of excess ligands **9** by washing with diethyl ether. Then partially functionalized nanocrystals, that is, nanocrystals containing at the same time remaining TOPO ligands and **9** on their surface (CdSe−**9**/TOPO), were extracted with chloroform. The fraction containing quasicompletely functionalized nanocrystals, CdSe−**9**, was only soluble in DMSO or thiophene. Hence the difference in solubility of the functionalized nanocrystals with respect to the initial and the partially functionalized ones can be used for a quantitative separation of these fractions.

Figure 6 shows the absorption spectra of the initial nanocrystals and of free thiophenedithiobenzoic acid **9**, in comparison with the corresponding hybrid fractions CdSe−**9**/TOPO and CdSe−**9**. The characteristic $\pi-\pi^*$ transition of the C═S at 360 nm[21] dominates the spectrum of **9** and also the one of the hybrid compound CdSe−**9**.

Further analytical evidence of the grafting reaction is given by proton NMR spectroscopy of **9** and CdSe−**9** (Figure 7). The peak of the carbodithioic acid proton at 6.3 ppm disappears in the spectrum of CdSe−**9**, consistent with the deprotonation of the acid function during the reaction. The positions of all peaks are low-field-shifted upon grafting on the nanocrystal surface, as electron density from the completely conjugated ligand is delocalized over the chelating bond formed between the sulfur atoms and a surface cadmium atom, resulting in a descreening effect. Additionally, a broadening of the peaks is observed resulting from the restricted motion of the grafted ligands.[27] This broadening is particularly pronounced for the protons located most closely to the nanocrystals' surface accounting for the signal at 8.4 ppm.

Photoluminescence (PL) investigations of the hybrid CdSe−**9** give information about possible photoinduced charge-transfer processes at the organic−inorganic interface. In Figure 8 the room-temperature PL spectra of the CdSe nanocrystals before and after functionalization with **9** are compared. In the latter case only a broad emission ranging from ca. 430 to 590 nm of very low intensity is detectable.

The efficient quenching of the nanocrystals' PL in the hybrid CdSe−**9** stands out against previous studies on oligothiophene-functionalized CdSe nanocrystals, in which a minimum oligomer length of 5 thiophene units has been determined for nearly complete PL extinction.[28] The different chemical nature of the anchor function, phosphonic acid in the reported case and carbodithioic acid in our study, is most probably at the origin of the observed changes in the PL

(27) (a) Kuno, M.; Lee, J. K.; Dabbousi, B. O.; Mikulec, F. V.; Bawendi, M. G. *J. Chem. Phys.* **1997**, *106* (23), 9869−9882. (b) Kalyuzhny, G.; Murray, R. W. *J. Phys. Chem. B* **2005**, *109* (15), 7012−7021.
(28) Milliron, D. J.; Alivisatos, A. P.; Pitois, C., Edder, C.; Fréchet, J. M. J. *Adv. Mater.* **2003**, *15* (1), 58−61.

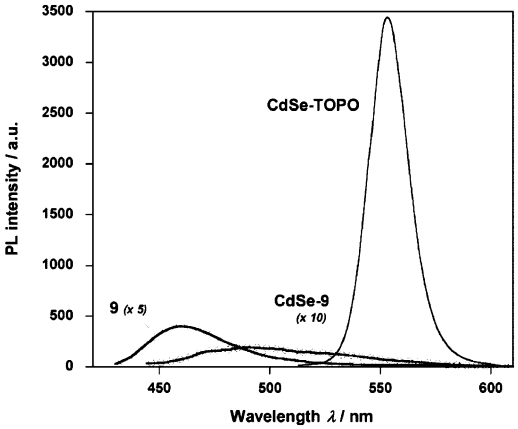

Figure 8. PL spectra of **9**, CdSe−TOPO, and CdSe−**9**, recorded in DMSO (excitation wavelength 400 nm).

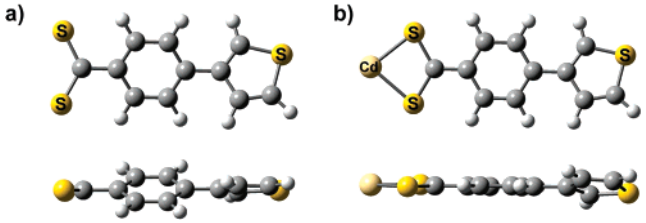

Figure 9. (a) Optimized structure of thiophenedithiobenzoate in its negative ion form; (b) optimized structure after complexation of a Cd^{2+} ion. Side views (bottom row) demonstrate the different torsion angles.

properties. To get a better understanding of the hybrid system, we optimized the geometry of a model consisting of a complex between a Cd^{2+} ion and a thiophenedithiobenzoate molecule by means of ab initio calculations in the framework of density functional theory[29] by use of the Becke−Perdew functional B3P86.[30] Cadmium was treated with the ECP (effective core potential) developed by Andrae et al.,[31] which describes the inner shells and includes relativistic corrections. For the outer electrons we used the same basis functions as Eichkorn and Ahlrichs[32] and the complete basis set used for Cd was ECP-2444G. Even though this restricted first-order model does not reflect accurately the binding situation on the surface of a CdSe nanocrystal, general trends can be deduced. Furthermore the validity of our model is confirmed by the calculated Cd−S atomic distances of 2.43 Å, which are in good agreement with the ones determined by single-crystal X-ray diffraction on mononuclear Cd−dithioate complexes.[33] Complexation of a cadmium ion has a striking impact on the structure of the carbodithioate ligand, whose planarity is strongly enhanced with respect to the free molecule (Figure 9). The dihedral angle between the carbodithioate group and the phenyl ring is reduced from 26.7° to 2.5°. It can also be noticed that the dihedral angle between the phenyl ring and the thiophene ring decreases from 32.6° to 16.2°. Therefore, a much better delocalization of the valence electrons over the entire molecule is expected, consistent with the observed changes

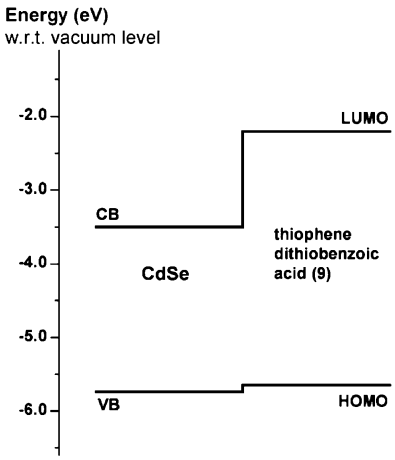

Figure 10. Electronic energy level alignment for 3.2 nm CdSe nanocrystals and compound **9**.

in the proton NMR spectrum of ligand **9** upon its grafting on the nanocrystals' surface (Figure 7) and with the slight bathochromic shift of its absorption spectrum (Figure 6).

Concerning the PL quenching mechanism, first of all the possibility of the creation of nonradiative decay channels during the ligand exchange has to be investigated. The emission of CdSe nanocrystals is very sensitive to surface functionalization and can significantly decrease when nonpassivated surface states are formed during the ligand exchange. However, our recent studies revealed that nanocrystals' fluorescence is clearly detectable after ligand exchange with an aliphatic carbodithioate such as tridecanedithioate.[5] This ligand contains the same anchor group as **9** but a nonconjugated aliphatic radical. Therefore it can be concluded that the observed fluorescence quenching in CdSe−**9** is a consequence of either energy or charge transfer between the nanocrystal and the aromatic ligand, inhibiting radiative recombination of the photocreated excitons. Unfortunately, the ab initio calculations of our simple model, in which **9** is bound to an isolated cadmium ion, do not allow us to further elucidate the photophysical behavior of the hybrid: they cannot provide correct values of the HOMO and LUMO levels of **9** on the nanocrystal surface, as the calculated energy levels depend strongly on the charge of the cadmium ion and therefore on its chemical environment.

Further insight can be obtained by exploiting the results of optical spectroscopy. Energy transfer from ligand **9** to the nanocrystal can be ruled out as a possible quenching mechanism due to the higher optical energy gap of the former, determined as 3.4 eV from its absorption spectrum. Energy transfer from the nanocrystal to the ligand, in turn, is not possible as there is no overlap between the emission spectrum of the used nanocrystals (Figure 8) and the absorption spectrum of **9** (Figure 6). Using the electrochemically estimated HOMO level of **9**, a tentative energy level diagram of CdSe−**9** can be proposed (Figure 10). Although there is some uncertainty about the absolute positions of the energy levels, our results suggest a staggered (type II) alignment in the hybrid CdSe−**9**. Therefore, after photoexcitation a charge-separated state results as a consequence of hole transfer from the nanocrystal to the carbodithioate or electron transfer from the carbodithioate to the nanocrystal,

(29) Kohn, W.; Becke, A. D.; Parr, R. G. *J. Phys. Chem.* **1996**, *100*, 12974.
(30) Becke, A. D. *Phys. Rev. A.* **1988**, *38* (6), 3098−3100.
(31) Andrae, D.; Häussermann, U.; Dolg, M.; Stoll, H.; Preuss, H. *Theor. Chim. Acta* **1990**, *77* (2), 123−141.
(32) Eichkorn, K.; Ahlrichs, R. *Chem. Phys. Lett.* **1998**, *288*, 235.
(33) O'Brien, P.; Walsh, J. R.; Watson, I. M.; Motevalli, M.; Henriksen, L. *J. Chem. Soc., Dalton Trans.* **1996**, 2491−2496.

respectively. Photoinduced electron transfer is the most probable mechanism, providing a rapid relaxation channel competing with radiative recombination and thus strongly reducing the photoluminescence intensity of **9** (cf. Figure 8).

CdSe−**9** can in principle be used—either directly or in blends with polythiophene—as active species in photovoltaic devices. A drawback is, however, the relatively low solubility of the hybrid, which is limited to DMSO, thiophene, or similar solvents. On the other hand, the solubility can be strongly enhanced when longer, alkyl-substituted oligo- or polythiophenes such as compounds **10** or **11** are used. Furthermore, as the conjugation length influences the position of the HOMO level of the organic moiety, this allows at the same time for the tuning of the relative position of the energy levels of the two semiconductors in the hybrid with the goal to facilitate charge transfer and minimize recombination processes. Spectroscopic and morphological studies of these systems are currently underway.

Conclusion

To summarize, we functionalized in a three-step procedure thiophene-based oligomers and polymers with carbodithioic acid groups, and the spectroscopic properties as well as the electrochemical behavior of the resulting compounds were characterized. The interest of these molecules lies in their potential for the surface functionalization of semiconductor nanocrystals. This has been demonstrated by exchanging the initial surface ligands of CdSe nanocrystals (TOPO) with 4-thiophen-3-yldithiobenzoic acid (**9**) under mild conditions. Spectroscopic studies revealed charge transfer upon photoexcitation at the organic/inorganic interface of this hybrid compound, resulting in an efficient extinction of the photoluminescence. Because of the high affinity of carbodithioic acid-substituted oligo- and polythiophenes for metals and semiconductors, these molecules are well-suited for the functionalization of a large variety of nanoparticles and surfaces. The control of the organic/inorganic interface on the molecular level can be a way to overcome problems encountered in simple blends of the two components (i.e. conjugated oligomers or polymers and semiconductor nanocrystals), which have been used in thin film solar cells.[3e,f] Uncontrolled phase segregation is inhibited through the chemical binding provided by the carbodithioate group. Furthermore, by changing the conjugation length of the organic backbone, the energy levels in the hybrid compounds can be optimized in order to enhance charge transfer and minimize recombination processes.

Acknowledgment. We thank Professor A. Pron for fruitful discussions, Professor S. Sadki for providing the facility of electrochemical measurements and Dr. J. Bleuse for help with photoluminescence spectroscopy.

CM061105P